Zeitschrift für Kristallographie 207, 193–208 (1993)

The crystal structure of wolframite type tungstates at high pressure

J. Macavei and H. Schulz

Institut für Kristallographie und Mineralogie der Universität München,
Theresienstr. 41, D-80333 München, Germany

Received: March 18, 1992; in final form: September 14, 1992

High pressure / Tungstates / Wolframites / Crystal structure

Abstract. Single-crystal structure determinations of wolframite-type structures were performed using a diamond anvil cell with beryllium gaskets. Unit cell parameters of $MgWO_4$, $MnWO_4$ and $CdWO_4$ were determined at several pressures up to 8.0 GPa and structure refinements were performed up to 6.0 GPa. The high pressure behaviour is compared with the behaviour of the related scheelite-type structure.

All investigated compounds compress anisotropically with the *b*-axis 1.5 to 2.5 times more compressible than the *c*-axis and 1.2 to 2.1 times more compressible than the *a*-axis.

In all compounds, the WO_6 polyhedra are significantly less compressible than the AO_6 octahedra; the compressions of the latter are comparable with the bulk compressions of the compounds. Anisotropies in the pressure response of the AO_6 and WO_6 polyhedra result in the anisotropic unit-cell compression.

With increasing pressure the oxygen atomic positions remain constant within one standard deviation, while the heavy atoms positions show a different pressure dependence: a shift of y(Mg) to smaller values and of y(Cd) to higher values, while y(Mn) undergoes little if any change.

With increasing pressure the A and W cations approach each other, indicating a tendency of a transition from the wolframite structure to the scheelite structure, where the A and W cations lie in the same plane.

Introduction

ABO_4 compounds crystallize in different structure types according to the size and charge of the cations. Most molybdates and tungstates of divalent

---

Correspondence to: J. Macavei, Inst. für Kristallographie und Mineralogie der Universität München, Theresienstr. 41, 80333 München, Germany.

cations crystallize either in the scheelite-type or in the wolframite-type structure. While tungstates and molybdates of larger cations ($r_A > 0.90$ Å) crystallize in the scheelite structure, the tungstates of smaller cations ($r_A < 0.90$ Å) and the high pressure phases of molybdates are stable in the wolframite structure. The Cd compounds have a special position: $CdWO_4$ crystallizes in the wolframite type, $CdMoO_4$ in the scheelite type. The mole volumes of both components are nearly identical (Sleight, 1972).

High pressure investigations on scheelite-type structures have been already performed by Hazen, Finger and Mariathson (1985). They determined the change of the lattice parameters under pressure for $CaWO_4$, $CaMoO_4$, $PbWO_4$, $PbMoO_4$ and $CdMoO_4$ and also performed a single-crystal structure determination for the calcium compounds up to 5.7 GPa.

Single-crystal structure studies at high pressure were performed previously in diamond anvil cells suitable for structures with high symmetry. We recently developed an improved pressure cell (Koepke, Dietrich, Glinnemann and Schulz, 1985) with beryllium gaskets (Macavei and Schulz, 1990) which allows the investigation of structures with low symmetry up to 10 GPa. It is therefore possible for the first time to investigate the monoclinic structure of the wolframites at high pressure.

In this work, a comparison is made between the high pressure behaviour of the two related structures, the wolframite and the scheelite structure.

The high pressure behaviour of the investigated tungstates can be explained with the polyhedral approach of Hazen and Finger (1982).

Experimental

Specimen

Single crystals of $MgWO_4$, $MnWO_4$ and $CdWO_4$ were prepared by the flux growth method (Wilke, 1963; Schulze, Wilke and Waligora, 1967). Mixtures of proper proportions of $Mg(Mn,Cd)WO_4$ and of mixed melts of $Na_2WO_4 - WO_3 - Mg(Mn,Cd)O$ were heated at 1050° C for 12 h before cooling down at a rate of 12° C/h. The grown crystals were separated by chemical leaching with NaOH and NH_3 solutions out of the flux. Most of the crystals were 30 μm to 1 mm in size. The crystals used for the experiments had sizes of approximately $30 \times 60 \times 70$ μm.

Data collection

All measurements were carried out with an Enraf-Nonius CAD4 four-circle diffractometer using monochromatic MoK_α radiation.

Diffraction intensities were first collected outside the diamond-anvil cell by the ω-scan technique. To find out systematic errors caused by the pressure cell, room-pressure data were also collected within the diamond-anvil cell.

The high-pressure measurements were carried out in a diamond anvil cell (Koepke et al., 1985; Ahsbahs, 1984) developed at the Max Planck Institut in Stuttgart (MPI cell) with beryllium gaskets (Brush Wellman S-65A or I-70 grade). Details of cell preparation are given elsewhere (Macavei and Schulz, 1990). As pressure transmitting medium a mixture of 4:1 methanol – ethanol was used (Piermarini, Block and Barnett, 1973).

The pressure measurements were made by the ruby fluorescence method with an estimated error of ± 0.07 GPa (Piermarini, Block, Barnett and Forman, 1975).

Because there is no optical access to the sample chamber on the four-circle diffractometer it is not possible to center the crystal optically. Also, the centering method of Hamilton (1974), modified by King and Finger (1979), cannot be applied because only one half of the reciprocal space is accessible. The centering was regarded as sufficient if the four symmetrical equivalent reflections with $\chi = 0$ showed a θ-deviation smaller than 0.03°. Because of the high background scattering produced by the Be-gaskets and the steel parts of the pressure cell, a smaller collimator (ϕ = 0.5 mm) and a smaller detector split (2 mm) were used in order to gain a better signal to background ratio. Due to the small collimator and slit, as well as to the X-ray absorption in the lower diamond anvil, longer counting times (4 – 6 min) were necessary compared with a standard data collection. In order to always get the same number of reflections the θ-range was extended gradually with increasing pressure.

For each compound, diffraction data were collected at four pressures including ambient pressure, up to approximately 6.0 GPa. At the highest applied pressure of about 8.0 GPa the crystal was destroyed because the gasket became too thin. It was possible, however, to determine the unit cell parameters at this pressure. Due to the imperfect centering of the crystal in the MPI cell, the lattice parameters show great deviations. Therefore they were also determined in a Merill-Bassett type cell (Merill and Bassett, 1974) (MB cell). The unit cell parameters as a function of pressure are listed in Table 1.

Data reduction

All reflections shadowed by the two pillars of the MPI cell (Ahsbahs, 1987), as well as those overlapping with reflections of the ruby or of the diamond crystals, were omitted. Reflections coinciding with beryllium or steel powder rings were also removed.

The paths of the primary and diffracted beams through the lower diamond and through the gasket were calculated, and the measured intensities were corrected with respect to the linear absorption coefficients of diamond

Table 1. Unit cell parameters of $MgWO_4$, $MnWO_4$ and $CdWO_4$ at various pressures (e. s. d. in parentheses).

P (GPa)	a (Å)	b (Å)	c (Å)	β (°)	V (Å)^3
			$MgWO_4$		
0.0001	4.696(2)	5.683(2)	4.945(3)	90.83(5)	132.0(2)
0.0001 MPI cell	4.695(1)	5.6834(4)	4.9371(7)	90.93(2)	131.7(1)
0.0001 MB cell	4.688(1)	5.6755(6)	4.9274(8)	90.72(2)	131.1(1)
1.05	4.674(1)	5.657(2)	4.9180(4)	90.70(2)	130.0(1)
2.44	4.658(1)	5.637(1)	4.9050(4)	90.65(2)	128.8(1)
3.02	4.660(1)	5.6406(1)	4.910(1)	90.64(2)	129.1(1)
3.91	4.643(1)	5.620(2)	4.8933(5)	90.60(2)	127.7(1)
4.82	4.637(1)	5.610(1)	4.887(4)	90.61(2)	127.1(1)
4.86	4.636(1)	5.6123(6)	4.889(1)	90.57(2)	127.2(1)
5.61	4.621(2)	5.597(1)	4.880(1)	90.54(4)	126.2(1)
5.90	4.624(1)	5.594(2)	4.880(1)	90.56(2)	126.2(1)
6.02	4.617(2)	5.591(1)	4.876(1)	90.52(4)	125.9(1)
6.54	4.613(2)	5.587(1)	4.872(1)	90.48(3)	125.6(1)
7.90	4.604(1)	5.5748(9)	4.862(2)	90.49(3)	124.8(1)
			$MnWO_4$		
0.0001	4.830(1)	5.7603(9)	4.994(1)	91.14(2)	138.8(1)
0.0001 MPI cell	4.8277(8)	5.761(1)	4.997(8)	91.14(1)	139.0(1)
0.0001 MB cell	4.832(2)	5.761(1)	4.9986(5)	91.17(3)	139.1(1)
0.81	4.818(2)	5.7445(6)	4.9893(6)	91.23(3)	138.1(1)
1.83	4.808(2)	5.7295(7)	4.9824(8)	91.19(4)	137.2(1)
2.81	4.798(2)	5.7106(7)	4.9738(9)	91.22(4)	136.2(1)
4.75	4.780(2)	5.681(1)	4.960(1)	91.18(2)	134.7(2)
5.00	4.7766(8)	5.681(2)	4.9605(9)	91.19(2)	134.6(1)
5.46	4.771(2)	5.669(1)	4.9537(8)	91.21(5)	133.9(1)
5.93	4.762(3)	5.660(2)	4.9507(7)	91.23(4)	133.4(1)
8.42	4.7401(4)	5.627(1)	4.9342(9)	91.32(2)	131.6(1)
			$CdWO_4$		
0.0001	5.028(5)	5.862(2)	5.067(2)	91.50(5)	149.3(2)
0.0001 MPI cell	5.031(3)	5.8573(9)	5.0709(8)	91.50(3)	149.4(1)
0.0001 MB cell	5.0255(8)	5.860(2)	5.0724(8)	91.51(1)	149.3(1)
0.82	5.015(1)	5.839(2)	5.066(1)	91.53(2)	148.3(1)
1.75	5.008(2)	5.818(7)	5.061(2)	91.57(3)	147.4(3)
2.45	5.001(1)	5.809(4)	5.0536(8)	91.67(2)	146.8(2)
2.81	5.011(2)	5.804(2)	5.050(1)	91.62(2)	146.9(1)
3.51	4.992(1)	5.788(4)	5.0454(8)	91.73(2)	145.7(2)
4.32	4.975(3)	5.765(2)	5.037(1)	91.84(2)	144.5(2)
4.55	4.982(1)	5.768(5)	5.039(1)	91.83(2)	144.7(2)
5.43	4.977(2)	5.752(4)	5.031(1)	91.94(2)	143.9(2)
6.37	4.966(3)	5.720(3)	5.025(1)	92.04(3)	142.6(2)
8.20	4.953(2)	5.705(3)	5.011(1)	92.30(3)	141.6(2)

Table 2. Details of structure determination.

P (GPa)	Max. $\sin\theta/\lambda$ (Å^{-1})	Number of reflections				R_{int} (%)	R_w (%)	R (%)
		meas.	used	independent				
				all	$F > 3\sigma(F)$			
				$MgWO_4$				
0.0001	0.7035	1482	1464	392	392	6.97	2.77	2.45
0.0001 MPI cell	0.7035	777	603	336	312	4.85	4.87	4.28
3.02	0.7099	778	722	334	311	5.88	3.95	3.81
4.86	0.7120	780	524	319	298	9.54	4.92	4.16
5.90	0.7141	777	429	326	295	5.31	4.26	4.17
				$MnWO_4$				
0.0001	0.7035	1574	1547	408	406	6.07	3.82	3.23
0.0001 MPI cell	0.7035	856	667	402	375	5.67	4.96	4.66
2.81	0.7077	849	635	402	366	6.43	4.60	4.29
5.00	0.7141	866	660	342	314	12.22	6.08	5.66
5.93	0.7247	892	726	394	357	6.14	5.51	5.51
				$CdWO_4$				
0.0001	0.7035	1632	1632	431	430	5.99	4.51	3.56
0.0001 MPI cell	0.7035	903	652	418	389	7.73	5.68	5.30
2.81	0.7099	911	704	414	380	7.40	5.52	4.95
4.32	0.7162	915	708	431	353	13.19	12.75	11.65
6.37	0.7183	917	749	427	364	9.29	8.48	7.21

and beryllium (Hazen, 1976; Finger and King, 1978). An analytical correction for the absorption by the crystal sample (the absorption coefficients of the compounds for the MoK_α radiation are: $MgWO_4$ $-469\ cm^{-1}$, $MnWO_4$ $-486\ cm^{-1}$, $CdWO_4$ $-475\ cm^{-1}$) was also necessary. Finally, Lorentz and polarization corrections were applied. Details of the structure determination and of the intensity measurement are recorded in Table 2.

Structure refinements

All structures were refined in space group $P2/c$ using the program SHELX76 (Sheldrick, 1976). A weighting scheme of $1/(\sigma(F) + 0.0002F^2)$ was used for reflections with $F > 3\sigma(F)$. All other reflections were given small weights. Atomic form factors for neutral atoms were used (International Tables IV, 1974).

The A-atoms occupy the positions $2(f)$ $1/2,y,1/4$, the W-atoms the positions $2(e)$ $0,y,1/4$. The eight oxygen atoms lie on two symmetrical different positions $4(g)$ x,y,z. Because of the low precision in refining the anisotropic thermal parameters from the data collected within the cell, only isotropic ones were refined. Alltogether, fourteen parameters were refined, including a scale factor and an isotropic extinction factor.

The structure parameters at ambient conditions, refined from the data collected out of the cell, are consistent with the results of other authors (Morell, Cantrell and Chang, 1980; Filipenko, Pobedimskaia, Ponomarev and Belov, 1969; Weitzel, 1966; Dachs, Stoll and Weitzel, 1967; Chichagov, Ilyukhin and Belov, 1966). A good agreement exists between the room pressure parameters refined from the data collected within and without the pressure cell. Deviations greater than one s.d. were noticed only for the thermal parameters of the cations in the $CdWO_4$. Sometimes a repeated recentering of the reflections used for the orientation matrix was necessary due to a slight motion of the crystal. This repeated recentering could explain the bad refinement for $CdWO_4$ at 4.32 GPa. The high-pressure atomic parameters were compared with the refined parameters from the data collected at room pressure in the cell. The results of the refinements are given in Table 3[1].

Results and discussions

Compressibilities

The investigated compounds compress anisotropically, with the *b*-axes 1.5 to 2.5 times more compressible than the *c*-axes, and 1.2 to 2.1 times more compressible than the *a*-axes. The anisotropy of compressibility increases with increasing ionic radius.

The similarity between the wolframite and the scheelite structure is illustrated in Figure 1. A feature not shown in the figure is that the consecutive wolframite cells are sheared by $(a + c)/2$ when they are stacked up along *b*-axis to form the scheelite structure. The *b*-axis in the wolframite structure corresponds to the *c*-axis in the scheelite structure, both of them the directions of the largest compressibility. In the scheelite-type compounds the *c*-axes are 1.2 to 1.9 times more compressible than the *a*-axes (see Hazen, Finger and Mariathson, 1985).

The bulk moduli K [144(3) GPa for $MgWO_4$, 131(2) GPa for $MnWO_4$, 136(5) GPa for $CdWO_4$] calculated from the Birch-Murnagham equation of state with $K' = 4$ (Hazen and Finger, 1982) show that wolframite structures are less compressible than the investigated scheelite structures: $K = 64(2)$ for the two Pb-compounds, $K = 104(2)$ for $CdMoO_4$, $K = 68(9)$ for $CaWO_4$ and $K = 82(1)$ for $CaMoO_4$.

---

[1] Additional material to this paper can be ordered from the Fachinformationszentrum Karlsruhe GmbH, D-76344 Eggenstein-Leopoldshafen, Germany. Please quote reference no. CSD 57001, the names of the authors and the title of the paper.

Table 3. Atomic parameters of $MgWO_4$, $MnWO_4$ and $CdWO_4$ at various pressures (e. s. d. in parentheses).

			$MgWO_4$			
P (GPa)		0.0001	0.0001 MPI cell	3.02	4.86	5.90
Mg	*y*	0.6742(6)	0.675(1)	0.673(1)	0.671(1)	0.672(1)
	U (Å^2)	0.0079(6)	0.008(1)	0.010(1)	0.007(1)	0.008(1)
W	*y*	0.1819(1)	0.1818(1)	0.1825(1)	0.1832(2)	0.1834(2)
	U (Å^2)	0.0052(2)	0.0061(4)	0.0063(3)	0.0055(3)	0.0053(3)
O_1	*x*	0.216(1)	0.220(3)	0.220(2)	0.223(3)	0.219(2)
	y	0.107(1)	0.106(2)	0.106(1)	0.106(2)	0.107(2)
	z	0.937(1)	0.935(2)	0.939(2)	0.935(2)	0.938(2)
	U (Å^2)	0.0084(9)	0.010(2)	0.008(2)	0.010(2)	0.010(2)
O_2	*x*	0.256(1)	0.255(3)	0.256(2)	0.255(3)	0.255(2)
	y	0.3766(9)	0.377(2)	0.378(1)	0.380(2)	0.382(2)
	z	0.397(1)	0.401(2)	0.401(2)	0.401(2)	0.402(2)
	U (Å^2)	0.0070(9)	0.008(2)	0.006(1)	0.005(2)	0.009(2)

			$MnWO_4$			
P (GPa)		0.0001	0.0001 MPI cell	2.81	5.00	5.93
Mn	*y*	0.6856(4)	0.6849(6)	0.6849(6)	0.687(1)	0.6853(9)
	U (Å^2)	0.0108(4)	0.0105(6)	0.0104(6)	0.0108(8)	0.0094(7)
W	*y*	0.1800(1)	0.1800(1)	0.1811(1)	0.1815(2)	0.1821(2)
	U (Å^2)	0.0060(2)	0.0062(3)	0.0062(3)	0.0062(4)	0.0051(4)
O_1	*x*	0.211(1)	0.211(2)	0.213(2)	0.210(3)	0.213(3)
	y	0.102(1)	0.102(2)	0.102(2)	0.107(3)	0.106(3)
	z	0.943(1)	0.941(2)	0.943(2)	0.941(3)	0.942(3)
	U (Å^2)	0.010(1)	0.009(2)	0.011(2)	0.013(3)	0.010(2)
O_2	*x*	0.250(1)	0.250(2)	0.250(2)	0.251(3)	0.250(3)
	y	0.374(1)	0.375(2)	0.376(2)	0.381(3)	0.381(3)
	z	0.393(1)	0.392(2)	0.394(2)	0.392(3)	0.392(2)
	U (Å^2)	0.011(1)	0.011(2)	0.011(2)	0.008(3)	0.009(3)

			$CdWO_4$			
P (GPa)		0.0001	0.0001 MPI cell	2.81	4.32	6.37
Cd	*y*	0.6977(1)	0.6979(3)	0.6987(3)	0.6988(8)	0.7014(6)
	U (Å^2)	0.0125(3)	0.0105(4)	0.0109(4)	0.018(11)	0.0136(7)
W	*y*	0.1785(1)	0.1784(2)	0.1801(2)	0.1811(5)	0.1827(3)
	U (Å^2)	0.0085(2)	0.0061(4)	0.0072(4)	0.0122(9)	0.0098(6)
O_1	*x*	0.203(1)	0.203(2)	0.201(2)	0.192(7)	0.204(4)
	y	0.098(1)	0.096(2)	0.096(2)	0.094(6)	0.093(4)
	z	0.949(1)	0.952(2)	0.951(2)	0.958(6)	0.955(4)
	U (Å^2)	0.012(1)	0.011(2)	0.012(2)	0.018(7)	0.014(4)
O_2	*x*	0.242(1)	0.241(1)	0.241(2)	0.233(6)	0.239(4)
	y	0.372(2)	0.371(2)	0.374(2)	0.376(6)	0.379(3)
	z	0.383(1)	0.382(2)	0.383(2)	0.388(6)	0.384(4)
	U (Å^2)	0.0115(9)	0.012(2)	0.012(2)	0.016(7)	0.009(4)

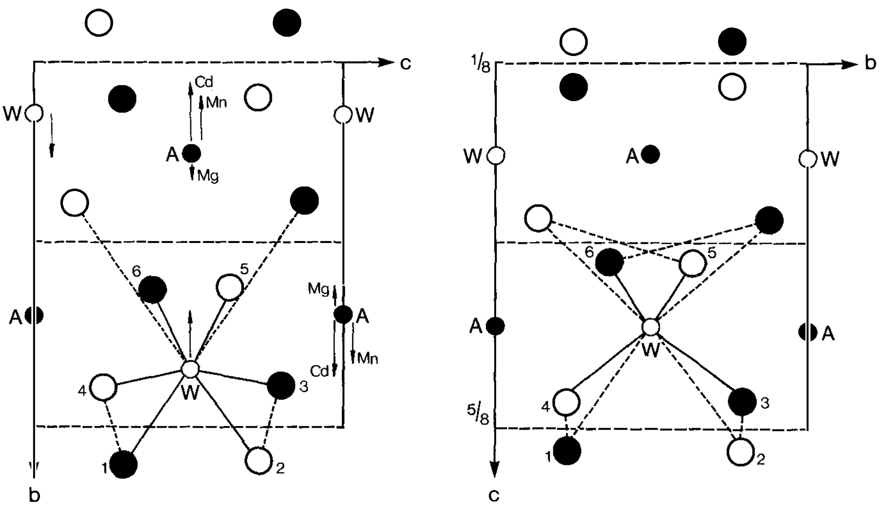

Fig. 1. Wolframite structure (left) compared to a portion of scheelite structure (right). Small full circles: A cations at 1/2, small open circles: Mo or W cations at 0, large open circles: oxygens at 1/4 and large full circles: oxygens at −1/4 (Sleight, 1972). The arrows indicate the atomic shifts under pressure.

High pressure crystal structure

The wolframite structure can be described as a distorted hexagonal close packing of O atoms (Dachs, Stoll and Weitzel, 1967; Cid-Dresdner and Escobar, 1968) with A and W atoms each occupying one-fourth of the octahedral voids. The distorted octahedra containing cations of only one type form infinite zig-zag chains extended along the *c* axis. Like octahedra are joined by edges, different octahedra by corners (see Fig. 2).

Hazen and Finger (1982) developed a polyhedral approach to describe the crystal structure change under pressure. They characterize the compression of a structure by means of the behaviour of individual polyhedra, which build up the crystal structure.

According to this approach, the anisotropic cell edge compressibilities can be correlated with the behaviour of the structure polyhedra. The lowest compressibility along the chain direction (*c*-axis) is related to the small variation of the A−A and W−W distances (see Tables 4−6). Chains of AO_6 and WO_6 octahedra, alternate along the *b*-axis, the direction of the largest compressibility. The nearing of the AO_6 and WO_6 polyhedra through their compression and distortion results in a clear shortening of the A−W distances (2% for $MgWO_4$, 1.4% for $MnWO_4$, 1.8% for $CdWO_4$).

The decrease of the oxygen-oxygen bonds under pressure is also visible from Tables 4−6. The O−O bonds in the AO_6 polyhedra compress more

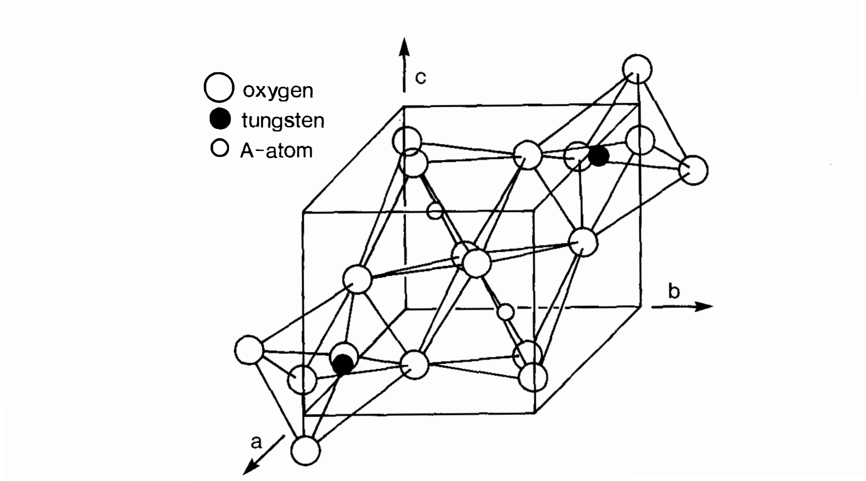

Fig. 2. Wolframite crystal structure (Morell, Cantrell and Chang, 1980).

Table 4. Bond distances (Å) in $MgWO_4$.

P (GPa)	0.0001 MPI cell	3.02	4.86	5.90
W–Mg	3.651(6)	3.608(4)	3.586(5)	3.577(6)
W–Mg	3.475(2)	3.457(1)	3.447(2)	3.441(2)
Mg–Mg	3.165(9)	3.127(7)	3.109(8)	3.104(1)
W–W	3.213(1)	3.198(1)	3.192(1)	3.187(1)
W–O_2[2]*	1.79(1)	1.774(9)	1.77(1)	1.78(1)
W–O_1[2]	1.92(1)	1.896(9)	1.91(1)	1.88(1)
W–O_1[2]	2.13(1)	2.124(9)	2.12(1)	2.12(1)
O_1–O_2[2]	2.77(1)	2.74(1)	2.75(1)	2.75(2)
O_1–O_2[2]	2.83(2)	2.81(1)	2.82(2)	2.79(2)
O_1–O_2[2]	2.75(1)	2.73(1)	2.73(1)	2.74(1)
O_2–O_2[1]	2.80(2)	2.79(2)	2.77(1)	2.77(1)
O_1–O_1[2]	2.48(2)	2.45(2)	2.47(3)	2.43(2)
O_1–O_1[2]	2.74(1)	2.725(7)	2.71(1)	2.72(1)
O_1–O_1[1]	2.73(2)	2.74(2)	2.73(2)	2.72(2)
Mg–O_1[2]	2.03(1)	2.03(1)	2.01(1)	2.02(1)
Mg–O_2[2]	2.08(1)	2.063(8)	2.06(1)	2.053(9)
Mg–O_2[2]	2.18(1)	2.15(1)	2.12(1)	2.11(1)
O_1–O_2[2]	3.00(1)	2.98(2)	2.97(1)	2.97(1)
O_1–O_2[2]	3.05(3)	3.05(4)	3.03(3)	3.04(2)
O_1–O_2[2]	2.94(2)	2.92(2)	2.89(2)	2.87(1)
O_1–O_1[1]	3.21(2)	3.21(2)	3.15(2)	3.19(1)
O_2–O_2[2]	2.83(1)	2.812(8)	2.79(9)	2.77(1)
O_2–O_2[2]	2.85(2)	2.82(2)	2.80(2)	2.78(2)
O_2–O_2[1]	2.75(2)	2.72(2)	2.72(2)	2.72(2)

* Bracketed figures represent bond multiplicity.

Table 5. Bond distances (Å) in $MnWO_4$.

P (GPa)	0.0001 MPI cell	2.81	5.00	5.93
W–Mn	3.737(3)	3.713(3)	3.683(5)	3.684(4)
W–Mn	3.524(1)	3.504(1)	3.485(1)	3.479(1)
Mn–Mn	3.280(4)	3.263(4)	3.264(7)	3.244(7)
W–W	3.244(1)	3.235(1)	3.222(2)	3.220(2)
W–O_2[2]*	1.79(1)	1.77(1)	1.78(1)	1.77(1)
W–O_1[2]	1.92(1)	1.91(1)	1.89(1)	1.90(1)
W–O_1[2]	2.13(1)	2.13(1)	2.13(2)	2.13(1)
O_1–O_2[2]	2.75(1)	2.74(1)	2.73(2)	2.72(2)
O_1–O_2[2]	2.86(1)	2.85(1)	2.83(2)	2.83(2)
O_1–O_2[2]	2.77(1)	2.74(1)	2.79(3)	2.78(2)
O_2–O_2[1]	2.78(2)	2.76(2)	2.76(3)	2.74(2)
O_1–O_1[2]	2.43(2)	2.43(2)	2.42(3)	2.44(3)
O_1–O_1[2]	2.758(9)	2.75(9)	2.76(3)	2.75(1)
O_1–O_1[1]	2.76(2)	2.78(2)	2.73(3)	2.75(3)
Mn–O_1[2]	2.10(1)	2.09(1)	2.06(2)	2.05(1)
Mn–O_2[2]	2.16(1)	2.15(1)	2.15(1)	2.15(1)
Mn–O_2[2]	2.27(1)	2.26(1)	2.23(2)	2.22(1)
O_1–O_2[2]	3.14(2)	3.11(1)	3.10(2)	3.09(2)
O_1–O_2[2]	3.17(2)	3.15(1)	3.14(1)	3.14(2)
O_1–O_2[2]	3.03(1)	3.00(2)	2.92(1)	2.91(2)
O_1–O_1[1]	3.41(1)	3.38(1)	3.39(2)	3.36(1)
O_2–O_2[2]	2.88(1)	2.86(1)	2.82(2)	2.81(1)
O_2–O_2[2]	2.99(2)	2.97(2)	2.91(3)	2.92(1)
O_2–O_2[1]	2.83(2)	2.82(2)	2.79(3)	2.80(1)

* Bracketed figures represent bond multiplicity.

than the O–O bonds in the WO_6 polyhedra. In the scheelite structure the decrease of the O–O bond distances of the eight-coordinated Ca polyhedra are a bit larger (2.5–4.3%). The W or Mo tetrahedra in the scheelites are rigid structural elements, that means, their O–O distances do not change significantly under pressure.

Hazen and Finger (1979) found an empirical relationship for predicting the polyhedral bulk modulus of oxides and silicates:

$$K_p = 750\ Z_c/d^3$$

where Z_c is the cation's formal charge and d is the mean cation-anion bond distance.

For the AO_6 octahedra with mean A–O distances 2.08–2.29 Å, K_p is approx. 150 GPa. This value is consistent with the observed bulk modulus $K_{obs} = V_0(P-P_0)/(V-V_0)$ of approx. 100 GPa. The WO_6 polyhedra with mean W–O distances of about 1.93 Å are significantly less compressible than the AO_6 polyhedra, with great deviations between K_p (approx.

Table 6. Bond distances in $CdWO_4$.

P (GPa)	0.0001 MPI cell	2.81	4.32	6.37
W–Cd	3.774(2)	3.748(2)	3.732(5)	3.712(3)
W–Cd	3.597(2)	3.571(2)	3.555(4)	3.532(3)
Cd–Cd	3.437(3)	3.420(2)	3.416(7)	3.412(4)
W–W	3.287(1)	3.278(1)	3.275(4)	3.271(2)
W–O_2[2]*	1.77(1)	1.77(1)	1.74(3)	1.75(2)
W–O_1[2]	1.91(1)	1.90(1)	1.85(3)	1.90(2)
W–O_1[2]	2.15(1)	2.13(1)	2.12(3)	2.12(2)
O_1–O_2[2]	2.71(2)	2.72(2)	2.71(4)	2.71(3)
O_1–O_2[2]	2.90(2)	2.88(2)	2.81(7)	2.89(3)
O_1–O_2[2]	2.77(2)	2.75(2)	2.74(4)	2.73(3)
O_2–O_2[1]	2.74(2)	2.73(2)	2.67(6)	2.69(4)
O_1–O_1[2]	2.39(2)	2.36(2)	2.26(7)	2.35(4)
O_1–O_1[2]	2.77(1)	2.76(1)	2.75(3)	2.73(2)
O_1–O_1[1]	2.86(2)	2.81(2)	2.79(7)	2.84(4)
Cd–O_1[2]	2.20(1)	2.19(1)	2.22(3)	2.17(2)
Cd–O_2[2]	2.28(1)	2.27(1)	2.26(3)	2.26(2)
Cd–O_2[2]	2.42(1)	2.39(1)	2.41(3)	2.37(2)
O_1–O_2[2]	3.317(8)	3.309(7)	3.361(8)	3.291(8)
O_1–O_2[2]	3.324(8)	3.303(7)	3.310(9)	3.314(8)
O_1–O_2[2]	3.151(7)	3.103(7)	3.086(9)	3.055(9)
O_1–O_1[1]	3.668(8)	3.666(7)	3.769(9)	3.648(9)
O_2–O_2[2]	2.95(1)	2.92(1)	2.90(3)	2.87(2)
O_2–O_2[2]	3.21(1)	3.16(1)	3.19(3)	3.13(2)
O_2–O_2[1]	2.96(1)	2.95(1)	3.04(3)	2.96(2)

* Bracketed figures represent bond multiplicity.

600 GPa) and K_{obs} (approx. 200 GPa). The differences between the calculated and the observed bulk moduli for the WO_6 polyhedra indicate that the empirical formula of Hazen and Finger may not be generally valid.

The K_{obs} values compared with the bulk moduli of the respective compounds are in agreement with results of the polyhedral approach: structures consisting primarily of edge-linked polyhedra have a bulk modulus that is less than or equal to that of the least compressible polyhedron (Hazen and Finger, 1979).

In the scheelite structure the CaO_6 polyhedra (K_p = 80 GPa, K_{obs} = 70 GPa) are more compressible than AO_6 polyhedra in the wolframite structure; the WO_6 polyhedra are practically incompressible (K_p = 800 GPa, $K_{obs} > 500$ GPa).

The oxygen positional parameters in the unit cell of wolframites do not change within one standard deviation (see Table 3). On the contrary, the parameters of the heavy atoms show a pressure dependence represented in Figures 3 and 4. For all investigated tungstates y(W) increases with increasing pressure, while A atoms show a different behaviour: y(Mg) shifts to

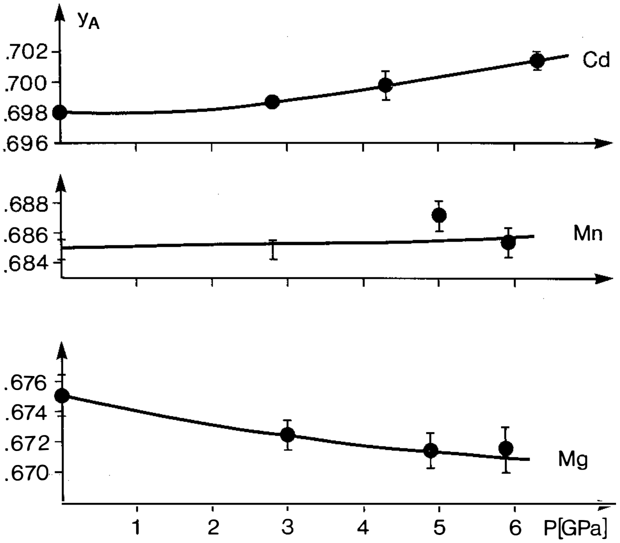

Fig. 3. y(A) parameters of the compounds versus pressure.

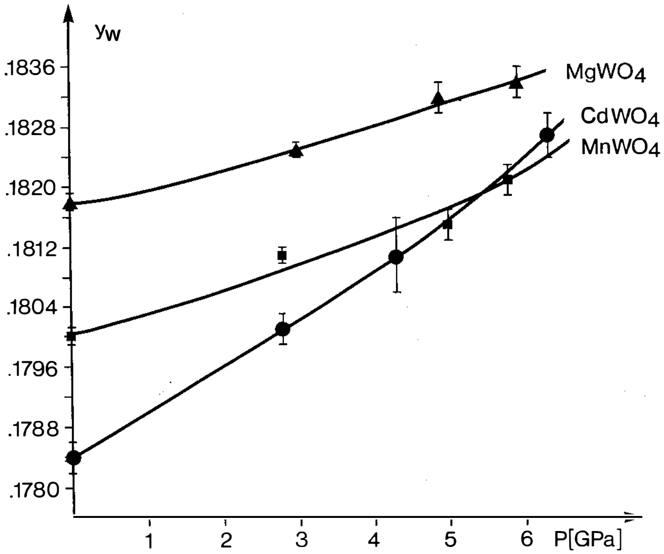

Fig. 4. y(W) parameters of the compounds versus pressure.

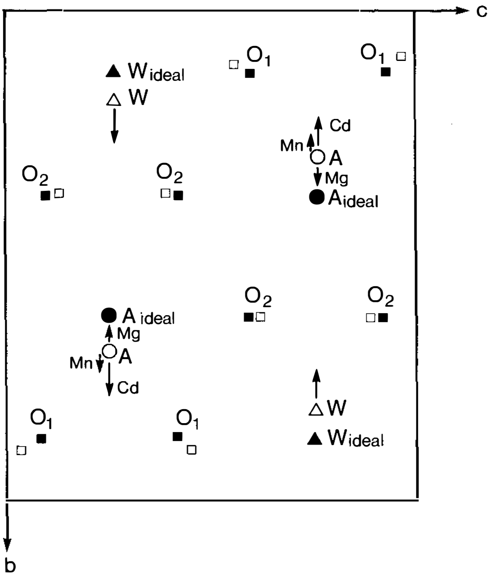

Fig. 5. Ideal and real atomic positions in the wolframite cell. ■: ideal oxygen position, □: real oxygen position.

smaller values, y(Cd) to higher values, and y(Mn) undergoes little if any change.

The behaviour can be correlated with the distortion of the hexagonal close packing. The cell constants and the atomic positional parameters for a calculated ideal close packing are:

$c/b = \sqrt{3}/2$
$a/b = \sqrt{2}/\sqrt{3}$
$a/c = 2\sqrt{2}/\sqrt{3}$

	x	y	z
A	0.5	0.625	0.25
W	0	0.125	0.25
O_1	0.25	0.125	0.9166
O_2	0.25	0.375	0.4166

The arrangement of ideal and real atoms in the unit cell (*bc*-plane) is shown in Figure 5; the arrows indicate the cation shift directions under pressure. The Mg atoms approach the position in an ideal close packing, the Cd and much less the Mn atoms move away from the ideal positions. The shifts are in concordance with the change of two distortion parameters which quantitatively describe the polyhedra distortion with increasing pressure (Robinson, Gibbs and Ribbe, 1971): the quadratic elongation

$$\langle\lambda\rangle = \sum_{i=1}^{n} (l_i/l_o)^2/n$$

Table 7. Volumes and distortion parameters for the AO_6 and WO_6 polyhedra.

			$MgWO_4$		
P (GPa)		0.0001 MPI cell	3.02	4.86	5.90
	V (Å^3)	11.978	11.756	11.505	11.414
MgO_6	$\langle\lambda\rangle$	1.018	1.015	1.013	1.015
	$\langle\sigma^2\rangle$	56.79	53.23	50.09	51.63
	V (Å^3)	9.442	9.206	9.267	9.154
WO_6	$\langle\lambda\rangle$	1.033	1.035	1.032	1.033
	$\langle\sigma^2\rangle$	94.17	97.79	93.11	95.61
			$MnWO_4$		
P (GPa)		0.0001 MPI cell	2.81	5.00	5.93
	V (Å^3)	13.361	13.082	12.621	12.564
MnO_6	$\langle\lambda\rangle$	1.011	1.025	1.031	1.028
	$\langle\sigma^2\rangle$	79.37	78.53	95.18	87.82
	V (Å^3)	9.387	9.277	9.280	9.264
WO_6	$\langle\lambda\rangle$	1.036	1.035	1.032	1.033
	$\langle\sigma^2\rangle$	101.79	102.24	97.66	96.25
			$CdWO_4$		
P (GPa)		0.0001 MPI cell	2.81	4.32	6.37
	V (Å^3)	15.465	15.064	15.365	14.708
CdO_6	$\langle\lambda\rangle$	1.034	1.037	1.035	1.038
	$\langle\sigma^2\rangle$	113.5	117.6	128.7	125.1
	V (Å^3)	9.294	9.145	8.672	8.998
WO_6	$\langle\lambda\rangle$	1.042	1.041	1.047	1.042
	$\langle\sigma^2\rangle$	115.80	120.46	134.25	124.37

(l_i: cation$-O_i$ distance, l_o: cation$-O_i$ distance of a regular polyhedron of the same volume, n: coordination number of the cation) and the bond angle variance

$$\langle\sigma^2\rangle = \sum_{i=1}^{n} (\theta_i - \theta_0)^2/(n-1)$$

(θ_i: bond angle in polyeder, θ_0: bond angle for a regular polyhedron).

The distortion parameters of the MgO_6 polyheder decrease with increasing pressure, while the same parameters of the MnO_6 and CdO_6 polyhedra become greater under pressure (see Table 7). The distortion parameters of the WO_6 polyhedra do not change significantly under pressure.

Demyanets, Ilyukhin, Ghicagov and Belov (1967) investigated the two related structures and the possibility of a morphotropic transition from wolframite to scheelite structure. They describe the "loosening" of the hexagonal close packing in the wolframite structure with increasing of cation radius, which finally leads to the change of the structure.

Table 8. Change of the A – W relative position along the *b*-axis with increasing pressure.

	A – W distance (Å)		
	Mg – W	Mn – W	Cd – W
Normal pressure	0.814(2)	0.778(2)	0.725(3)
Highest pressure	0.809(3)	0.750(2)	0.663(4)

Considering the relative position of the A and W cations along the *b* axis (Table 8) one can recognize the same transition tendency from the wolframite to the scheelite structure with increasing pressure (Fig. 1). With the exception of $MgWO_4$, where the change of the relative position of the cations is very small, there is an evident tendency of the Mn(Cd) and W atoms to approach each other. This means a change towards the scheelite structure where the A and W atoms lie in the same plane.

Conclusions

1. High pressure induce structural variations in the investigated tungstates.
2. The slight decrease of the A – A and W – W distances and a visible shortening of the A – W distances with increasing pressure result in the anisotropic unit-cell compression.
3. The structural variations that occur with changes in pressure are mainly associated with the AO_6 polyhedra.
4. With increasing pressure there is a recognizable transition tendency from the wolframite structure to the related scheelite structure.

Acknowledgment. This work was supported by the Deutsche Forschungsgemeinschaft (Schu 601/2-3).

References

Ahsbahs, H.: Diamond-anvil high-pressure cell for improved single-crystal X-ray diffraction measurements. Rev. Sci. Instrum. **55** (1984) 99 – 102.

Ahsbahs, H.: X-ray diffraction of single crystals at high pressure. Cryst. Growth Charact. **14** (1987) 263 – 302.

Chichagov, A. P., Ilyukhin, V. V., Belov, N. V.: Crystal structure of $CdWO_4$. Sov. Phys.-Dokl. **11** (1966) 11 – 13.

Cid-Dresdner, Hilda, Escobar, Carmen: The crystal structure of Ferberite, $FeWO_4$. Z. Kristallogr. **127** (1968) 61 – 72.

Dachs, H., Stoll, E., Weitzel, H.: Kristallstruktur und magnetische Ordnung des Hübnerits, $MnWO_4$. Z. Kristallogr. **125** (1967) 120 – 129.

Demyanets, L. N., Ilyukhin, V. V., Ghicagov, A. V., Belov, N. V.: Crystal chemistry of isomorphous substitutions in divalent metal molybdates and tungstates. Inorganic materials, Izv. Akad. Nauk SSSR, Neorg. Mater. **3** (1967) 2221 – 2234.

Filipenko, O. S., Pobedimskaya, E. A., Ponomarev, V. I., Belov, N. V.: The crystal structure of magnesium tungstate $MgWO_4$. Sov. Phys.-Crystallogr. **13** (6) (1969) 933–935.

Finger, L. W., King, H.: A revised method of operation of the single-crystal diamond cell and refinement of the structure of NaCl at 32 kbar. Am. Mineral. **63** (1978) 337–342.

Hamilton, W. C.: Angle settings for four-circle diffractometers. In: *International Tables for X-ray Crystallographie, Vol. IV,* 273–289, Kynoch Press, Birmingham, England (1974).

Hazen, R. M.: Effect of temperature and pressure on the cell dimension and X-ray temperature factors of periclase. Am. Mineral. **61** (1976) 266–271.

Hazen, R. M., Finger, L. W.: Bulk modulus-volume relationship for cation-anion polyhedra. J. Geophys. Res. **84** (B 12) (1979) 6723–6728.

Hazen, R. M., Finger, L. W.: *Comparative Crystal Chemistry.* John Wiley & Sons, New York (1982).

Hazen, R. M., Finger, L. W., Mariathson, J. W. E.: High pressure crystal chemistry of scheelite type tungstates and molybdates. J Phys. Chem. Solids **46** (1985) 253–263.

International Tables for X-Ray Crystallography, Vol. IV, Kynoch Press, Birmingham, England (1974).

King, H., Finger, L. W.: Diffracted beam crystal centering and its applications to high pressure crystallography. J. Appl. Crystallogr. **12** (1979) 374–378.

Koepke, J., Dietrich, W., Glinnemann, J., Schulz, H.: Improved diamond anvil high pressure cell for single crystal work. Rev. Sci. Instrum. **56** (1985) 2114–2122.

Macavei, J., Schulz, H.: Be-Gaskets suitable for pressure up to 10 GPa. Rev. Sci. Instrum. **55** (1990) 99–102.

Merill, L., Bassett, W. A.: Miniature diamond anvil pressure cell for single crystal X-ray diffraction studies. Rev. Sci. Instrum. **45** (1974) 290–294.

Morell, D. J., Cantrell, J. S., Chang, L. L. Y.: Phase relations and crystal structures of Zn and Cd tungstates. J. Am. Ceram. Soc. **63** (1980) 261–264.

Piermarini, G. I., Block, S., Barnett, J. D.: Hydrostatic limits in liquids and solids to 100 kbar. J. Appl. Phys. **44** (1973) 5377–5382.

Piermarini, G. I., Block, S., Barnett, J. D., Forman, A.: Calibration of the pressure dependence of the R_1 ruby fluorescence line to 195 kbar. J. Appl. Phys. **46** (1975) 2774–2780

Robinson, K., Gibbs, G. V., Ribbe, P. H.: Quadratic elongation: a quantitative measure of distortion in coordination polyhedra. Science **172** (1971) 567–570.

Schulze, D., Wilke, K. Th., Waligora, Ch.: Zur Chemie in Schmelzlösungen, III. Darstellung kristalliner Wolframate $Me^{2+}WO_4$. Z. Anorg. Allg. Chem. **352** (1967) 184–191.

Sheldrick, G. M.: Program for crystal structure determination SHELX76 (1976) University of Cambridge.

Sleight, A. W.: Accurate cell dimensions for ABO_4 molybdates and tungstates. Acta Crystallogr. **B28** (1972) 2899–2902.

Weitzel, H.: Kristallstrukturverfeinerung von Wolframiten und Columbiten. Z. Kristallogr. **144** (1966) 238–258.

Wilke, K. Th.: *Methoden der Kristallzüchtung.* Verlag Harri Deutsch, Frankfurt/Main und Zürich (1963).